Enhanced confinement in diverted negative-triangularity L-mode plasmas in TCV

S. Coda[1], A. Merle[1], O. Sauter[1], L. Porte[1], F. Bagnato[1], J. Boedo[2], T. Bolzonella[3], O. Février[1], B. Labit[1], A. Marinoni[4], A. Pau[1], L. Pigatto[3], U. Sheikh[1], C. Tsui[1,2], M. Vallar[1], T. Vu[1] and the TCV Team‡

[1]Ecole Polytechnique Fédérale de Lausanne (EPFL), Swiss Plasma Center, EPFL SB SPC, Station 13, CH-1015 Lausanne, Switzerland

[2]Department of Aerospace and Mechanical Engineering, University of California, San Diego, La Jolla, CA 92093, USA

[3]Consorzio RFX, Corso Stati Uniti 4, 35127 Padova, Italy

[4]Plasma Science and Fusion Center, Massachusetts Institute of Technology, Cambridge, MA 02139, USA

E-mail: `stefano.coda@epfl.ch`

Abstract. The favourable confinement properties of negative-triangularity (NT) tokamak configurations were discovered in the TCV tokamak in the late 1990's and were documented over the two following decades, through investigations of predominantly electron-heated plasmas in limited topologies. The most recent experimental campaign in TCV has marked a leap forward, characterized by the development of a variety of diverted NT shapes that are robustly stable with basic Ohmic heating. The application of auxiliary heating, directed now at both electrons and ions (using electron-cyclotron resonance heating as well as neutral-beam injection), has enabled the achievement of record performances for L-mode plasmas, with normalized β values reaching 2.8 transiently (as well as 2 in steady state, but reverting to a limited configuration) and with comparable ion and electron temperatures. The systematic confinement enhancement with NT is confirmed in these experiments. The L-mode existence space is broader than at positive triangularity, with only sporadic transitions to H-mode observed up to 1.4-MW heating power regardless of the magnetic-field-gradient direction relative to the X-point. These experiments are planned to be continued with even higher power following a heating-source upgrade.

Keywords: Plasma, Nuclear fusion, Tokamak, TCV, Triangularity, Confinement, Stability

Submitted to: *Plasma Phys. Control. Fusion*

‡ See author list of S. Coda et al 2019 Nucl. Fusion **59** 112023

1. Introduction

The TCV tokamak [1, 2] (major radius R=0.88 cm, minor radius a=0.25 cm, plasma current $I_p \leq$1 MA, toroidal magnetic field $B_\phi \leq$1.54 T) was designed with the stated goal of enabling the generation of an extremely wide range of flux-surface shapes, thanks to a set of 16 independently-powered, external poloidal-field coils – in addition to two internal coils for fast stabilization of the axisymmetric instability [3]. A broad shaping scan, focusing particularly – for simplicity – on two low-order moments, the elongation and the triangularity, was carried out early on in the life of TCV [4, 5] and led to the first observation of significantly improved confinement with negative triangularity (NT) [6, 7], i.e., with a "D" shape pointing its nose towards the high-field side (HFS).

Until 2015 the only form of auxiliary heating available on TCV was Electron Cyclotron Resonance Heating (ECRH), albeit at a very high power level (up to 2.7 MW for a $\sim$ 1-m^3 plasma). Until recently, therefore, the investigation of NT focused on regimes with $T_e \gg T_i$; in addition, only limiter configurations were used. In these conditions it was systematically confirmed that NT yielded better confinement than positive triangularity (PT) [8]. Core fluctuation measurements then revealed that this confinement enhancement was accompanied by turbulence suppression [9, 10, 11], and first-principles theoretical studies with gyrokinetic codes provided partial insight into the origin of this phenomenon [12, 13].

The past few years have witnessed a resurgence of international interest in the NT configuration as a potential candidate for a nuclear-fusion reactor [14], partly because of the attenuation of concerns regarding its technical feasibility, partly also because of new results from DIII–D [15, 16] and ASDEX Upgrade [17] broadly confirming the TCV findings, and finally out of the increased perception of the need for ELM-free solutions. In this respect NT offers the option of a confinement level comparable to that of H–mode but operating in an intrinsically ELM-free L–mode regime.

This paper describes a surge of experimentation on TCV in 2020–2021 to further address the NT option, particularly in view of its applicability to a reactor design. Specifically, this work resulted in the development of a large variety of stable diverted NT shapes; and in the first exploration of NT plasmas with a broad range of T_i/T_e, including cases with $T_i > T_e$, thanks to the availability of neutral-beam injection (NBI). The L–H power threshold was also investigated to assess the existence range of an L–mode NT edge. Along the way, record L–mode performances were also recorded for TCV, as measured by metrics such as β_N and the energy confinement time. Throughout this study, the basic finding that confinement improves with NT was confirmed in these new shapes and new heating regimes.

The remainder of this paper is organized as follows: section 2 will present the development of diverted NT shapes, while section 3 will discuss the search for the L–H transition threshold; section 4 will touch on the ancillary phenomenon of a high-density front on the inner divertor leg in some of these scenarios; the L–mode confinement enhancement at negative triangularity will be treated in section 5 along with the

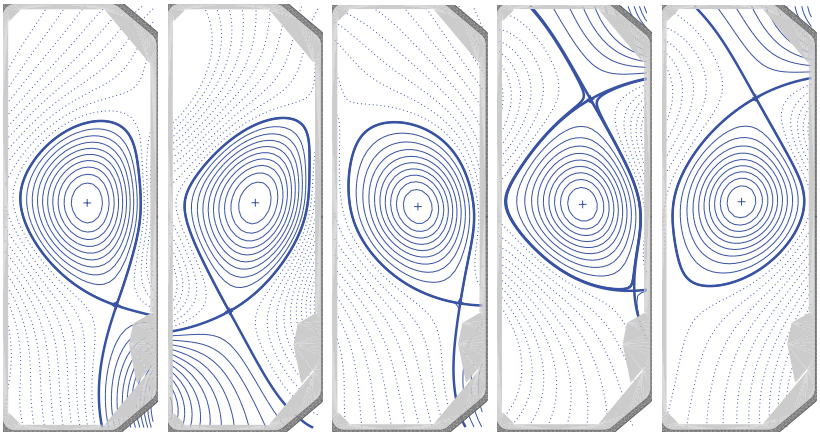

Figure 1: A selection of stable, diverted negative-triangularity configurations achieved in TCV.

attendant stability problems. Conclusions and an outlook will be offered in section 6.

2. The development of diverted negative-triangularity plasmas in TCV

The earliest attempts to create diverted NT shapes in TCV were plagued by macroscopic stability problems, particularly tearing modes and vertical displacement events (VDEs). For pragmatic reasons, hybrid lower-single-null (LSN) shapes were then developed with the lower half of the plasma featuring standard, positive triangularity, while the upper triangularity was varied from positive to negative. This led in particular to the first deliberate studies of a NT H-mode regime [18].

In the most recent campaign a concerted effort was made to find a stable, fully diverted, fully NT operating space at low edge safety factor ($q_{95} = 2.6 - 3.4$). This effort was successful through a process of iterative optimization, involving in particular staying within a given elongation range (typically below 1.7) and allowing sufficiently small plasma-wall gaps, to maximize the passive stabilization provided by the conducting wall. Within this basic recipe, the versatility of the poloidal-field-coil system and the adaptability of the TCV discharge design tools [3] permitted the creation of a wide variety of NT shapes: these include LSN, upper-single-null (USN) and double-null (DN) configurations, as well as all manners of hybrid combinations with different upper and lower triangularities. Representative examples can be seen in Fig. 1 , while Fig. 2 depicts additional limited cases with unusual bespoke shapes. These figures do illustrate the almost limitless variety of detailed shaping achievable on TCV, but it should also be added that all these plasmas are robustly MHD-stable in Ohmic conditions.

With additional heating, whether ECRH or NBI, this stability can quickly be challenged as will be discussed in section 5. However, one important practical observation is that no harm to the LFS first-wall components was detected in these configurations even up to 1.4-MW heating. The LFS graphite tiles were not explicitly designed for high-power handling [19] and yet survived several hundred high-power

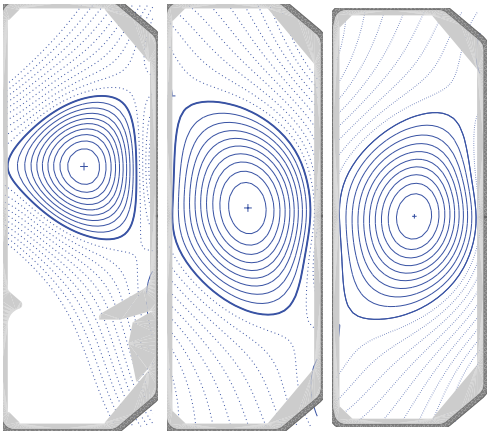

Figure 2: A selection of stable, limited negative-triangularity configurations achieved in TCV.

pulses – with an outer strike point placed on the LFS wall – entirely unscathed. It should be added that the vast majority of these shots were performed in the absence of the divertor baffles [20] that have now become a periodically recurrent feature of TCV.

3. L–mode resilience at negative triangularity

As discussed in the previous section, the shaping options in TCV are virtually unbounded. This is at the root of a certain amount of difficulty in establishing clear trends, as many variables can be varied independently over broad ranges. The only systematic study of diverted, H-mode NT plasmas in any tokamak, for instance, was performed in TCV by keeping the lower triangularity (on the X-point side) positive, and varying only the upper triangularity [18]. In these conditions, no evidence of a difference in the L–H power threshold was observed, and the H–mode could be sustained regularly and reliably with constant heating power while changing the upper triangularity, albeit reaching only modest negative values. This work showed that NT could be beneficial even in H–mode, resulting in less virulent ELMs that were more frequent and also expelled less energy [18]. This result was explained by the application of the EPED pedestal model [21], which indicated that NT closed off access to the second ballooning-stable region and thus caused instability to develop sooner during the pedestal growth, ultimately limiting its height and correspondingly reducing the ELM's impact.

The present work sought to characterize the L–H threshold power as a function of basic plasma parameters in fully NT, diverted plasmas. Up to 1.3 MW NBI power and 2.3 MW second-harmonic X-mode ECRH power were available, although their simultaneous application was practically precluded in most cases by their different optimal target densities. Out of several hundred shots with various power levels, with both directions of the ∇B drift, only a few entered into H–mode, rendering the achievement little more than anecdotal.

Figure 3 shows a comparison among three representative discharges: a positive-

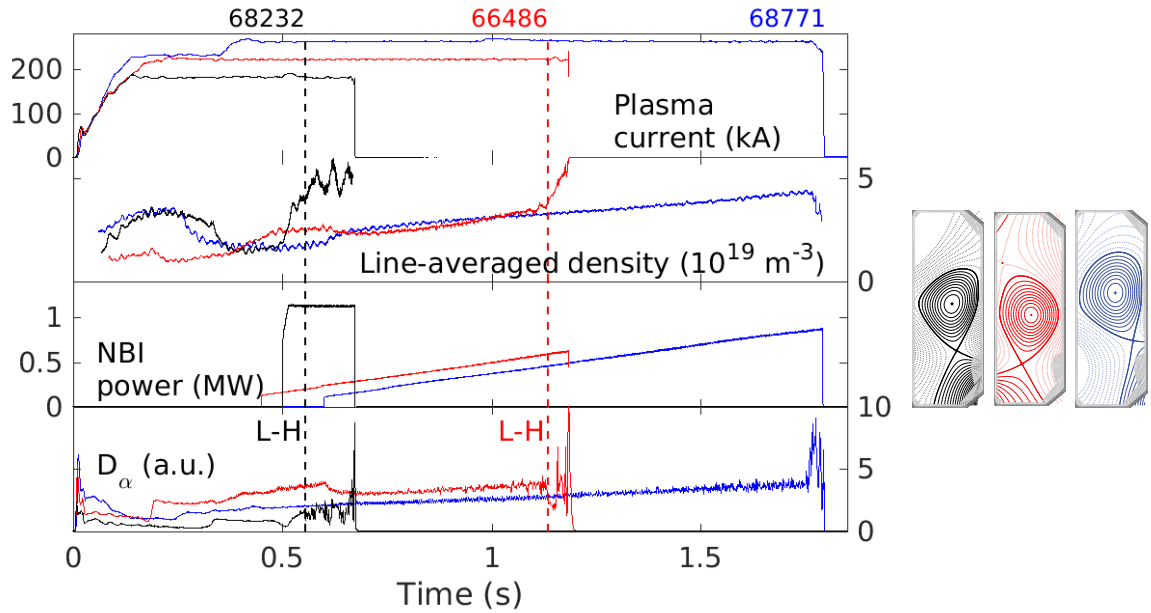

Figure 3: Comparison of three discharges: NT with L-H transition (black); PT with L-H transition (red); NT without L-H transition (blue).

and an otherwise similar negative-triangularity shot, both featuring slow power ramps, result respectively in an L–H transition at $\sim$ 0.6-MW power and in no transition all the way to 0.9 MW; while the third example, also at NT, does achieve H–mode through the instantaneous application of 1.1-MW NBI power – although a disruptive instability quickly ensues.

The general conclusion from this campaign is that H–mode is highly elusive at NT. It is clear from previous work, however, that some hybrid NT/PT configurations do access H–mode easily [18]. A thorough analysis of the aggregate NT database will be necessary to disentangle the parametric dependences and attempt to draw quantitative conclusions about a possible L–H transition law. An extension of this investigation to even higher power will likely be required to provide such a scaling with more solid statistical grounding. By the same token, the earlier findings on the suppression of the second-stability region [21] – related to the spatial distribution of the low-magnetic-shear region relative to the "bad-curvature" region – have been extended from the ELM characteristics in H–mode to the H–mode accessibility itself [22]; but no systematic investigation of this hypothesis has yet been carried out.

Auxiliary power will be further increased in TCV as a result of ECRH and NBI upgrades. It is expected that the L–H power threshold can be probed further, at higher power, in the next campaign. Part of the added ECRH power will be available at the third harmonic, still in X-mode, enabling access to higher-density plasmas generally compatible also with NBI heating. It will therefore become possible to explore heating regimes never attempted before.

4. High-density divertor front

In NT diverted plasmas, a region of elevated density is seen to form along the inner divertor leg in the common-flux region of the scrape-off layer (SOL). In extreme cases, the peak density in this region is found to exceed the peak density in the plasma core, as exemplified in Fig. 4. These extreme cases are found to occur in particular with high ECRH power. In fact, this effect has precluded access to higher core densities which may facilitate ingress into H–mode. In practice, increased gas puffing only causes more accumulation of plasma in the divertor leg, without any significant penetration into the core plasma.

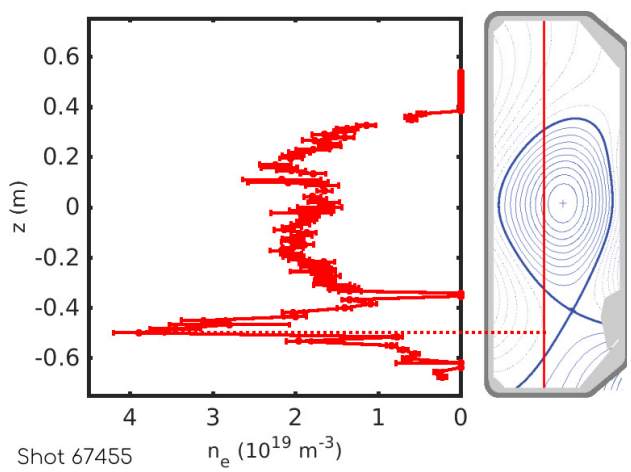

Figure 4: Density distribution along a vertical chord for a plasma heated with ECRH, highlighting a divertor-leg high-density front.

Smaller, but still measurable accumulation of density in the inner leg occurs with NBI heating as well. A quantitative characterization of this phenomenon is one of the goals of the analysis currently underway. This will likely require the establishment of a statistically relevant database with a meaningful, reduced set of descriptive parameters within the large variety of shapes achieved.

High-density HFS fronts, near the inner target, have been observed also on ASDEX Upgrade [23] and DIII–D [24]. Differences in ion orbital losses between PT and NT plasmas [25] could potentially be related to these observations. However, a complete, fundamental understanding of this phenomenon is still missing.

5. Confinement enhancement and stability issues for diverted negative-triangularity plasmas

In past TCV experiments with partially NT, diverted plasmas [18], the lower triangularity of LSN configurations was kept positive. The vast majority of past TCV data on the dependence of confinement on triangularity was obtained in limited configurations; this includes the earliest published scaling law that features an explicit dependence on the triangularity (δ), for plasmas heated by ECRH. This dependence was $\tau_{Ee} \propto (1+\delta)^{-0.35}$, where τ_{Ee} is the electron energy confinement time [7].

The development of fully NT diverted shapes, i.e., with negative *lower* triangularity, has now confirmed that the energy confinement time remains better in this configuration than in an equivalent positive-triangularity diverted plasma. A systematic investigation of the dependence of confinement on the detailed properties of the plasma shape is

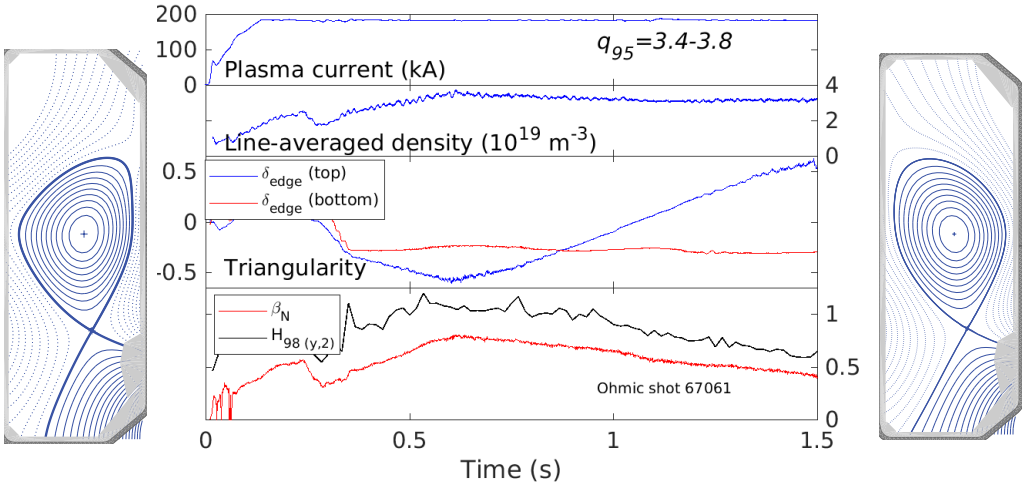

Figure 5: Ohmic shot: scan of the upper triangularity, while the lower triangularity – containing the X-point – is kept negative: (a) plasma current; (b) line-averaged density; (c) top and bottom trangularities; (d) β_N and $H_{98(y,2)}$ (the H-mode confinement enhancement factor). The safety-factor value q_{95} increases slightly with triangularity, from 3.4 to 3.8 during the scan.

beyond the scope of this article. However, the confinement enhancement at NT is illustrated by Figs. 5 and 6, in the cases of Ohmic heating and ECRH, respectively. In these examples the lower triangularity is kept constant and negative, while the upper triangularity is varied over a broad range during the discharge. It should be noted that no saturation or rollover of the confinement enhancement is observed, i.e., the confinement time keeps increasing down to the lowest values of δ that we have achieved. This is also confirmed in a limited scenario, as evidenced by Fig. 7.

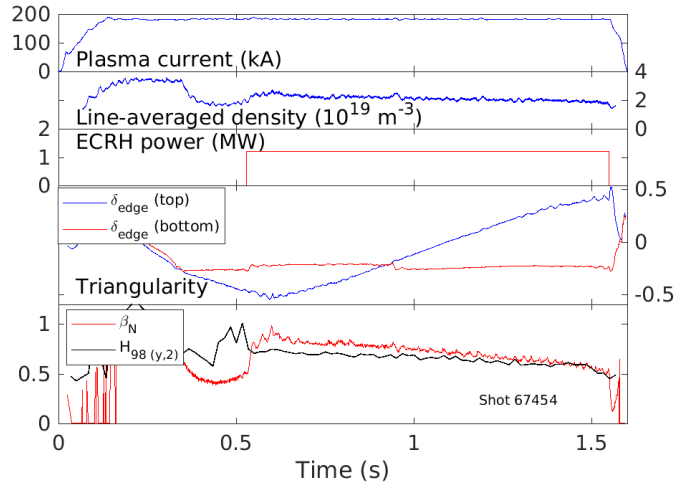

Figure 6: ECRH shot: scan of the upper triangularity, while the lower triangularity – containing the X-point – is kept negative: (a) plasma current; (b) line-averaged density; (c) ECRH power; (d) top and bottom trangularity; (e) β_N and $H_{98(y,2)}$ (the H-mode confinement enhancement factor).

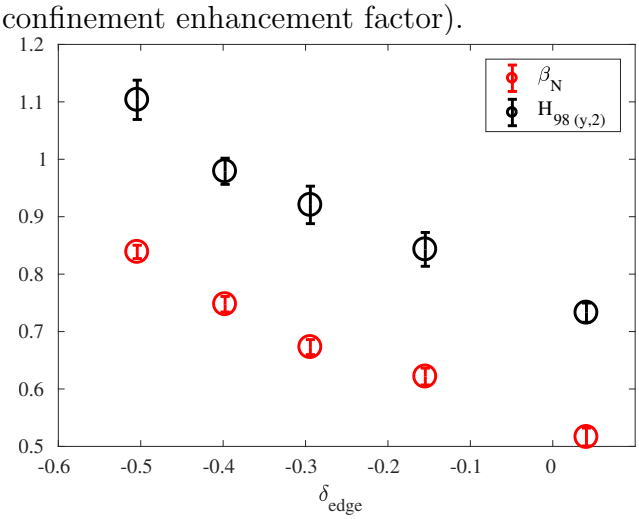

Figure 7: Ohmic shot (limited): β_N and $H_{98(y,2)}$ (the H-mode confinement enhancement factor) over a triangularity scan.

The clear connection of the NT confinement enhancement with turbulence suppression [10] has been extended more recently from the core to the SOL, where both Langmuir-probe measurements and gas-puff-imaging techniques have documented a dramatic reduction in both the fluctuation level and plasma-wall interaction as triangularity goes from positive to negative [26].

Another very important recent development has been the completion of the first full global, nonlinear gyrokinetic simulation of a PT vs a NT scenario, based on experimental TCV cases with identical (ECRH) power. Despite being gradient-driven, this simulation has broadly succeeded in reproducing the experimental heat flux in both cases - in other words, it has reproduced the confinement enhancement at NT [27]. Additionally, the calculated difference in the turbulent core density fluctuation amplitude between the two cases reproduces rather well the experimental results.

The attractiveness of a NT scenario as a potential reactor solution can be judged from the comparison shown in Fig. 8, featuring two roughly symmetrical positive- and negative-triangularity plasmas, both heated with NBI. The PT case is representative

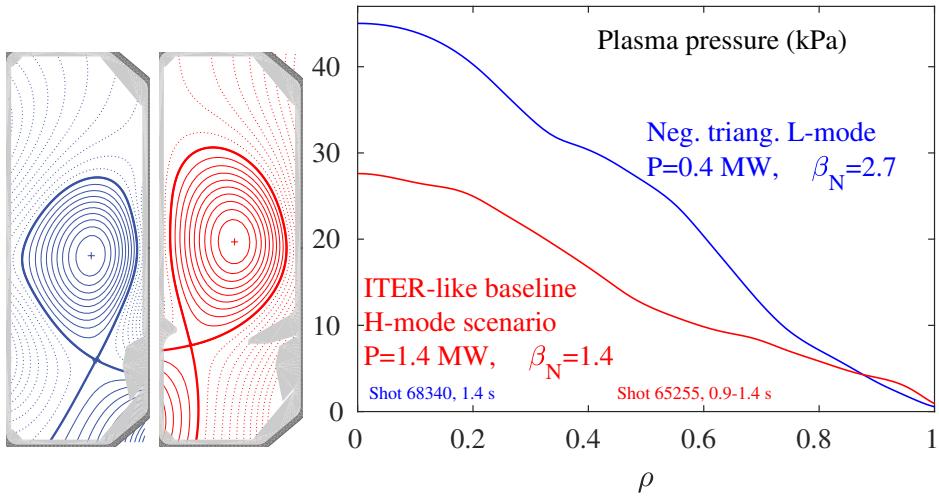

Figure 8: Flux-surface contours and pressure profile for ITER-like H–mode (red) and negative-triangularity L–mode (blue).

of the H–mode baseline scenario expected to be used in ITER. The NT case exhibits a smooth though more elevated pressure profile, notably lacking an edge pedestal, and is sustained at approximately twice the β_N value of the ITER case with only 30% of the auxiliary power.

However, it must be noted that the NT L–mode plasma shown here is not stationary and develops an ultimately disruptive instability. In the campaign that this paper is reporting on, no diverted, high-β_N *stationary* plasmas have been obtained with auxiliary heating, be it NBI or ECRH. A typical time history is shown in Fig. 9, which depicts the same NT discharge shown in Fig. 8, featuring a β_N value of 2.8 (in this case, the peak ion and electron temperatures are 2.0 keV and 1.2 keV, respectively). A rotating MHD mode invariably develops, starting at relatively low power values, and eventually leads to a disruption. In most cases, with edge safety factor $q_{95} < 4$, the mode is a neoclassical tearing mode (NTM) with poloidal and toroidal mode numbers $m = 2$ and $n = 1$, respectively. The disruption itself generally ultimately takes the form of a rapid vertical ($n = 0$) displacement, even for plasmas that are calculated to be intrinsically stable to the axisymmetric instability. With NBI it has also proven difficult to reach a stationary core density, whereas with ECRH the core density is rather resilient to change but the divertor high-density front discussed in section 4 tends to develop instead.

In limited plasmas high auxiliary power also leads to the appearance of NTMs, but stationary conditions have been reached in many cases and the loss of confinement caused by the NTM, if any, does not appear to be a major concern. An example is shown in Fig. 10, which depicts a stationary $\beta_N = 2$ phase (again with $T_i > T_e$: T_{i0}= 2.0 keV, T_{e0}= 1.3 keV). Analysis and modeling of this data set are ongoing to determine the exact nature of the instabilities and their dynamic development. It is believed that in most disruptive cases the disruption occurs at values of β_N that are below the ultimate β_N limit. This would offer hope for developing alternate, less disruptive paths, or

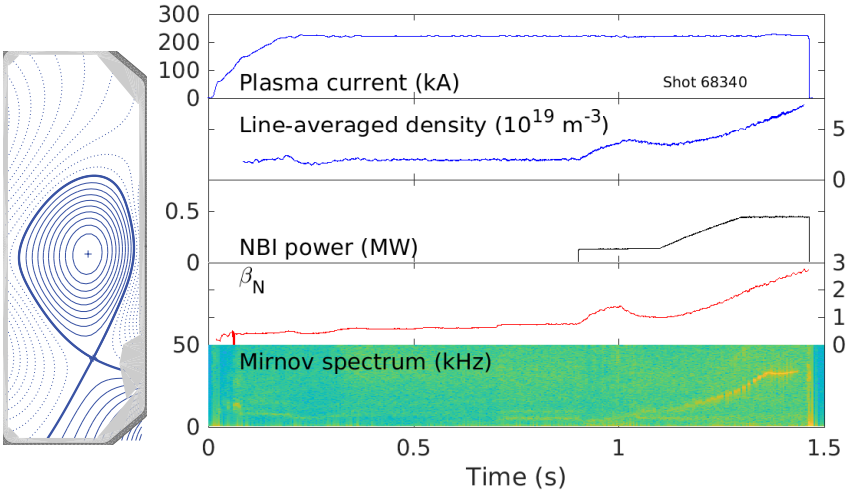

Figure 9: Flux-surface contours and time traces of (a) plasma current, (b) line-averaged density, (c) NBI power, (d) β_N, (e) magnetic-probe frequency spectrum, for shot 68340.

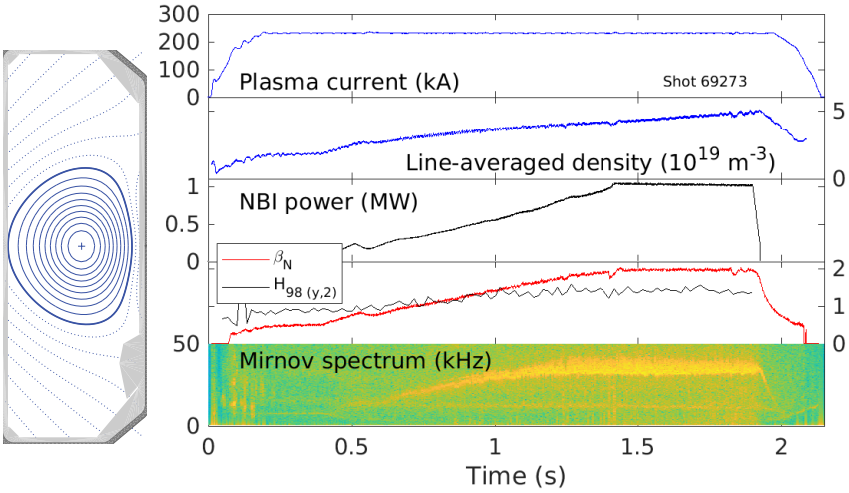

Figure 10: Flux-surface contours and time traces of (a) plasma current, (b) line-averaged density, (c) NBI power, (d) β_N and $H_{98(y,2)}$, (e) magnetic-probe frequency spectrum, for shot 69273.

for actively controlling the instabilities. Optimized current profile tailoring can also be explored, for instance steering NT plasmas into an advanced-tokamak regime with elevated safety-factor profiles which may also avoid the most virulent MHD modes [28].

Interestingly, according to preliminary indications the macroscopic current and density limits of NT plasmas do not appear to be significantly different from those of PT plasmas.

6. Conclusions and outlook

The addition of ion heating to TCV and a renewed worldwide interest in the negative-triangularity configuration as a possible candidate for a fusion reactor have spurred a sizable experimental campaign in 2020–2021 to develop, for the first time, stable diverted NT plasmas and push T_i/T_e to unity and above. A wide variety of diverted shapes have been obtained and a large database has been assembled on confinement and stability, in particular, but also on exhaust physics, fast-ion properties and edge turbulence.

While much detailed analysis still remains to be performed, some important general results have already emerged. One is the sheer capability of creating stable diverted plasmas with highly varying individual characteristics, and with no notable wall power-handling difficulties regardless of where the strike points are located. Another noteworthy conclusion is that the L–mode existence space is clearly wider at NT than at PT, and no systematic L–H power threshold has been identified up to 1.4 MW auxiliary heating with the ∇B direction pointing towards the X-point; this is a result that bodes well for a robust L–mode regime, which is the main current aspiration for negative-triangularity research. Finally, confinement is confirmed to be enhanced in these fully NT diverted configurations, relative to their PT counterparts; and confinement in fact increases continuously without saturation as the upper triangularity of a negative-lower-triangularity plasma goes to increasingly negative values.

In the process, record values of β_N have been established for TCV, although significant instability concerns remain and no stationary, high-β_N, diverted NT regime has as yet been obtained. Future work, also driven by ongoing analysis and modeling, will strive to find avenues to wholly or partly stabilize MHD instabilities – passively or actively – and achieve a better stationary performance that has been possible to date. Additional power, both NBI and ECRH, will also be available shortly, making it possible to test the L–mode boundary further. Part of the ECRH power will also be newly available at the third harmonic, which, thanks to its higher density cutoff, enjoys a wider range of applicability and can in particular be combined effectively with NBI. This will be an important new route for future investigations.

Acknowledgments

This work was supported in part by the Swiss National Science Foundation. This work has been carried out within the framework of the EUROfusion Consortium and has received funding from the Euratom research and training programme 2014-2018 and 2019-2020 under grant agreement number 633053. The views and opinions expressed herein do not necessarily reflect those of the European Commission.

[1] Hofmann F, Lister J B, Anton W, Barry S, Behn R, Bernel S, Besson G, Buhlmann F, Chavan R, Corboz M, Dutch M J, Duval B P, Fasel D, Favre A, Franke S, Heym A, Hirt A, Hollenstein C, Isoz P, Joye B, Llobet X, Magnin J C, Marletaz B, Marmillod P, Martin Y, Mayor J M, Moret J M, Nieswand C, Paris P J, Perez A, Pietrzyk Z A, Pitts R A, Pochelon A, Rage R, Sauter O, Tonetti G, Tran M Q, Troyon F, Ward D J and Weisen H 1994 *Plasma Physics and Controlled Fusion* **36** B277–B287 URL https://doi.org/10.1088/0741-3335/36/12b/023

[2] Coda S, Agostini M, Albanese R, Alberti S, Alessi E, Allan S, Allcock J, Ambrosino R, Anand H, Andrèbe Y, Arnichand H, Auriemma F, Ayllon-Guerola J, Bagnato F, Ball J, Baquero-Ruiz M, Beletskii A, Bernert M, Bin W, Blanchard P, Blanken T, Boedo J, Bogar O, Bolzonella T, Bombarda F, Bonanomi N, Bouquey F, Bowman C, Brida D, Bucalossi J, Buermans J, Bufferand H, Buratti P, Calabró G, Calacci L, Camenen Y, Carnevale D, Carpanese F, Carr M, Carraro L, Casolari A, Causa F, Čeřovský J, Chella O, Chmielewski P, Choi D, Christen N, Ciraolo G, Cordaro L, Costea S, Cruz N, Czarnecka A, Molin A D, David P, Decker J, Oliveira H D, Douai D, Dreval M, Dudson B, Dunne M, Duval B, Eich T, Elmore S, Embréus O, Esposito B, Faitsch M, Farník M, Fasoli A, Fedorczak N, Felici F, Feng S, Feng X, Ferró G, Février O, Ficker O, Fil A, Fontana M, Frassinetti L, Furno I, Gahle D, Galassi D, Galazka K, Gallo A, Galperti C, Garavaglia S, Garcia J, Garcia-Muñoz M, Garrido A, Garrido I, Gath J, Geiger B, Giruzzi G, Gobbin M, Goodman T, Gorini G, Gospodarczyk M, Granucci G, Graves J, Gruca M, Gyergyek T, Hakola A, Happel T, Harrer G, Harrison J, Havlíčková E, Hawke J, Henderson S, Hennequin P, Hesslow L, Hogeweij D, Hogge J P, Hopf C, Hoppe M, Horáček J, Huang Z, Hubbard A, Iantchenko A, Igochine V, Innocente P, Schrittwieser C I, Isliker H, Jacquier R, Jardin A, Kappatou A, Karpushov A, Kazantzidis P V, Keeling D, Kirneva N, Komm M, Kong M, Kovacic J, Krawczyk N, Kudlacek O, Kurki-Suonio T, Kwiatkowski R, Labit B, Lazzaro E, Linehan B, Lipschultz B, Llobet X, Lombroni R, Loschiavo V, Lunt T, Macusova E, Madsen J, Maljaars E, Mantica P, Maraschek M, Marchetto C, Marco A, Mariani A, Marini C, Martin Y, Matos F, Maurizio R, Mavkov B, Mazon D, McCarthy P, McDermott R, Menkovski V, Merle A, Meyer H, Micheletti D, Militello F, Mitosinkova K, Mlynář J, Moiseenko V, Cabrera P M, Morales J, Moret J M, Moro A, Mumgaard R, Naulin V, Nem R, Nespoli F, Nielsen A, Nielsen S, Nocente M, Nowak S, Offeddu N, Orsitto F, Paccagnella R, Palha A, Papp G, Pau A, Pavlichenko R, Perek A, Ridolfini V P, Pesamosca F, Piergotti V, Pigatto L, Piovesan P, Piron C, Plyusnin V, Poli E, Porte L, Pucella G, Puiatti M, Ptterich T, Rabinski M, Rasmussen J J, Ravensbergen T, Reich M, Reimerdes H, Reimold F, Reux C, Ricci D, Ricci P, Rispoli N, Rosato J, Saarelma S, Salewski M, Salmi A, Sauter O, Scheffer M, Schlatter C, Schneider B, Schrittwieser R, Sharapov S, Sheeba R, Sheikh U, Shousha R, Silva M, Sinha J, Sozzi C, Spolaore M, Stipani L, Strand P, Tala T, Biwole A T, Teplukhina A, Testa D, Theiler C, Thornton A, Tomaž G, Tomes M, Tran M, Tsironis C, Tsui C, Urban J, Valisa M, Vallar M, Vugt D V, Vartanian S, Vasilovici O, Verhaegh K, Vermare L, Vianello N, Viezzer E, Vijvers W, Villone F, Voitsekhovitch I, Vu N, Walkden N, Wauters T, Weiland M, Weisen H, Wensing M, Wiesenberger M, Wilkie G, Wischmeier M, Wu K, Yoshida M, Zagorski R, Zanca P, Zebrowski J, Zisis A and and M Z 2019 *Nuclear Fusion* **59** 112023 URL https://doi.org/10.1088/1741-4326/ab25cb

[3] Lister J, Hofmann F, Moret J, Buhlmann F, Dutch M, Fasel D, Favre A, Isoz P, Marltaz B, Marmillod P, Martin Y, Perez A and Ward D 1997 *Fusion Technology* **32**

[4] Moret J M, Franke S, Weisen H, Anton M, Behn R, Duval B P, Hofmann F, Joye B, Martin Y, Nieswand C, Pietrzyk Z A and van Toledo W 1997 *Phys. Rev. Lett.* **79**(11) 2057–2060 URL https://link.aps.org/doi/10.1103/PhysRevLett.79.2057

[5] Weisen H, Moret J M, Franke S, Furno I, Martin Y, Anton M, Behn R, Dutch M, Duval B, Hofmann F, Joye B, Nieswand C, Pietrzyk Z and Toledo W V 1997 *Nuclear Fusion* **37** 1741–1758 URL https://doi.org/10.1088/0029-5515/37/12/i07

[6] Pochelon A, Pietrzyk Z A, Goodman T P, Henderson M, Reimerdes H, Tran M, Behn R, Coda S, Dutch M J, Duval B P, Furno I, Hofmann F, Hogge J P, Lister J B, Llobet X, Martin Y, Moret J M, Nieswand C, Rommers J, Sauter O, van Toledo W, Tonetti G, Weisen H, Esipchuk Y V

and Martynov A A 1998 *2nd Europhysics Topical Conf. on RF Heating of Fusion Devices* **22A** 253

[7] Pochelon A, Goodman T, Henderson M, Angioni C, Behn R, Coda S, Hofmann F, Hogge J P, Kirneva N, Martynov A, Moret J M, Pietrzyk Z, Porcelli F, Reimerdes H, Rommers J, Rossi E, Sauter O, Tran M, Weisen H, Alberti S, Barry S, Blanchard P, Bosshard P, Chavan R, Duval B, Esipchuck Y, Fasel D, Favre A, Franke S, Furno I, Gorgerat P, Isoz P F, Joye B, Lister J, Llobet X, Magnin J C, Mandrin P, Manini A, Marlétaz B, Marmillod P, Martin Y, Mayor J M, Mlynar J, Nieswand C, Paris P, Perez A, Pitts R, Razumova K, Refke A, Scavino E, Sushkov A, Tonetti G, Troyon F, Toledo W V and Vyas P 1999 *Nuclear Fusion* **39** 1807–1818 URL https://doi.org/10.1088/0029-5515/39/11y/321

[8] Camenen Y, Pochelon A, Behn R, Bottino A, Bortolon A, Coda S, Karpushov A, Sauter O, Zhuang G and the TCV team 2007 *Nuclear Fusion* **47** 510–516 URL https://doi.org/10.1088/0029-5515/47/7/002

[9] Fontana M, Porte L, Coda S and and O S 2017 *Nuclear Fusion* **58** 024002 URL https://doi.org/10.1088/1741-4326/aa98f4

[10] Huang Z and and S C 2018 *Plasma Physics and Controlled Fusion* **61** 014021 URL https://doi.org/10.1088/1361-6587/aadb59

[11] Fontana M, Porte L, Coda S, Sauter O, Brunner S, Jayalekshmi A C, Fasoli A and and G M 2019 *Nuclear Fusion* **60** 016006 URL https://doi.org/10.1088/1741-4326/ab4d75

[12] Marinoni A, Brunner S, Camenen Y, Coda S, Graves J P, Lapillonne X, Pochelon A, Sauter O and Villard L 2009 *Plasma Physics and Controlled Fusion* **51** 055016 URL https://doi.org/10.1088/0741-3335/51/5/055016

[13] Merlo G, Fontana M, Coda S, Hatch D, Janhunen S, Porte L and Jenko F 2019 *Physics of Plasmas* **26** 102302 (*Preprint* https://doi.org/10.1063/1.5115390) URL https://doi.org/10.1063/1.5115390

[14] Kikuchi M, Takizuka T, Medvedev S, Ando T, Chen D, Li J, Austin M, Sauter O, Villard L, Merle A, Fontana M, Kishimoto Y and Imadera K 2019 *Nuclear Fusion* **59** 056017 URL https://doi.org/10.1088/1741-4326/ab076d

[15] Austin M E, Marinoni A, Walker M L, Brookman M W, deGrassie J S, Hyatt A W, McKee G R, Petty C C, Rhodes T L, Smith S P, Sung C, Thome K E and Turnbull A D 2019 *Phys. Rev. Lett.* **122**(11) 115001 URL https://link.aps.org/doi/10.1103/PhysRevLett.122.115001

[16] Marinoni A, Austin M E, Hyatt A W, Walker M L, Candy J, Chrystal C, Lasnier C J, McKee G R, Odstrčil T, Petty C C, Porkolab M, Rost J C, Sauter O, Smith S P, Staebler G M, Sung C, Thome K E, Turnbull A D and Zeng L 2019 *Physics of Plasmas* **26** 042515 (*Preprint* https://doi.org/10.1063/1.5091802) URL https://doi.org/10.1063/1.5091802

[17] Happel T, Puetterich T, Hobirk J, Zohm H and the ASDEX Upgrade Team 2020 *Bull. Am. Phys. Soc.* **65** TO10.00009

[18] Pochelon A, Angelino P, Behn R, Brunner S, Coda S, Kirneva N, Medvedev S Y, Reimerdes H, Rossel J, Sauter O, Villard L, Wagner D, Bottino A, Camenen Y, Canal G P, Chattopadhyay P K, Duval B P, Fasoli A, Goodman T P, Jolliet S, Karpushov A, Labit B, Marinoni A, Moret J M, Pitzschke A, Porte L, Rancic M, Udintsev V S and the TCV Team 2012 *Plasma and Fusion Research* **7** 2502148–2502148

[19] Chavan R, Pitts R, Hofmann F, Hollenstein C, Moret J M, Rage R and Tonetti G 1993 *FIRST WALL COMPONENTS FOR THE TCV TOKAMAK* pp 222–226 ISBN 9780444899958

[20] Reimerdes H, Duval B, Elaian H, Fasoli A, Février O, Theiler C, Bagnato F, Baquero-Ruiz M, Blanchard P, Brida D, Colandrea C, Oliveira H D, Galassi D, Gorno S, Henderson S, Komm M, Linehan B, Martinelli L, Maurizio R, Moret J M, Perek A, Raj H, Sheikh U, Testa D, Toussaint M, Tsui C, Wensing M, the TCV team and the EUROfusion MST1 team 2021 *Nuclear Fusion* **61** 024002 URL https://doi.org/10.1088/1741-4326/abd196

[21] Merle A, Sauter O and Medvedev S Y 2017 *Plasma Physics and Controlled Fusion* **59** 104001 URL https://doi.org/10.1088/1361-6587/aa7ac0

[22] Saarelma S, Austin M E, Knolker M, Marinoni A, Paz-Soldan C, Schmitz L and Snyder P B 2021 *Plasma Physics and Controlled Fusion* **63** 105006 URL https://doi.org/10.1088/1361-6587/ac1ea4

[23] Manz P, Potzel S, Reimold F, Wischmeier M and Team A U 2017 *Nuclear Materials and Energy* **12** 1152–1156 ISSN 2352-1791 proceedings of the 22nd International Conference on Plasma Surface Interactions 2016, 22nd PSI URL https://www.sciencedirect.com/science/article/pii/S2352179116300333

[24] Marinoni A, Austin M E, Hyatt A W, Saarelma S, Scotti F, Yan Z, Chrystal C, Coda S, Glass F, Hanson J, McLean A G, Pace D C, Paz-Soldan C, Petty C, Porkolab M, Schmitz L, Sciortino F, Smith S P, Thome K E and Turco F 2021 *Nuclear Fusion* URL http://iopscience.iop.org/article/10.1088/1741-4326/ac1f60

[25] Nishimura Y, Waelbroeck F L and Zheng L J 2020 *Physics of Plasmas* **27** 012505 (*Preprint* https://doi.org/10.1063/1.5131157) URL https://doi.org/10.1063/1.5131157

[26] Han W, Offeddu N, Golfinopoulos T, Theiler C, Tsui C, Boedo J, Marmar E and the TCV Team 2021 *Nuclear Fusion* **61** 034003 URL https://doi.org/10.1088/1741-4326/abdb95

[27] Merlo G, Huang Z, Marini C, Brunner S, Coda S, Hatch D, Jarema D, Jenko F, Sauter O and Villard L 2021 *Plasma Physics and Controlled Fusion* **63** 044001 URL https://doi.org/10.1088/1361-6587/abe39d

[28] Zheng L, Kotschenreuther M T, Waelbroeck F L, Austin M E, Rowan W L, Valanju P and Liu X 2018 *2018 IAEA Fusion Energy Conf. (Gandhinagar, India, 22–27 October 2018)* IAEA–CN–391/TH/P5–31